Micromachined Millimeter-Wave Cavity Resonators

K. J. Song* · B. S. Yoon* · J. C. Lee* · B. Lee* · J. H. Kim* ·
N. Y. Kim* · J. Y. Park** · G. H. Kim** · J. U. Bu** · K. W. Chung**

Abstract

In this paper, micromachined millimeter-wave cavity resonators are presented. One-port and two-port cavity resonators at Ka-band are designed using 3D design software, HP HFSS™ ver. 5.5. Cavity resonators are fabricated on Si substrate, which is etched down for the cavity, bonded with a Quartz wafer in which metal patterns for the feeding line and coupling slot are formed.

One-port resonator shows the resonant frequency of 39.34 GHz, the return loss of 14.5 dB, and the loaded Q (Q_L) of 150. Two-port cavity resonator shows the resonant frequency of 39 GHz, the insertion and return losses of 4.6 dB and 19.8 dB, the loaded (Q_L) and unloaded Q (Q_U) of 44.3 and 107, respectively.

Ⅰ. INTRODUCTION

In mobile communication systems, size, weight, and performance are critical trade-offs in system design. Many RF components are historically considered as the most problematic elements in terms of high density integration. Commercially available systems are under development at 28 GHz for the Local Multi-point Distribution System (LMDS), and also a telecommunication band at Ka-Band[1],[2]. Waveguide components are widely used at these frequencies and offer very good performance. However, they have many problems such as size, weight and cost.

As one of solutions to overcome these problems, MEMS (Micro-Electro-Mechanical System) has been introduced to microwave and millimeter wave circuit. The application of this technology in high frequency RF circuits has resulted in low-loss, high-performance transmission lines, high Q factor resonator, and other passive components. With the maturity of micromachined techniques in fabrication of microwave circuits, it is now possible to make miniature silicon micromachined waveguides or cavities.

In this paper, the bulk micro-machining technique for building high-Q and low loss resonator at millimeter-wave frequency is discussed. Especially, bulk micro-machining do not suffer from dielectric and dispersion loss at this frequency, and has the advantage of the monolithic microwave/millimeter wave intergrated circuit fabrication process[3]. In spite of many advantages of the MEMS, the RF component design of using MEMS is very difficult due to the lack of the proper simulation tools. This paper shows that the passive components using the micro-machining have the good characteristic in relative with the conventional technique and have possibility to construct the components at the millimeter wave

「This work was supported by MEMS program in G7 projects funded by the Ministry of Science & Technology and the Ministry of Industry, Commerce, and Energy.」

* RFIC Research and Education Center & Mission Technology Research Center, Kwangwoon University, 447-1 Wolgye-dong, Nowon-ku, Seoul 139-701, Korea

** Microsystem and RF Team, Materials and Device Laboratory, LG Electronics Institute of Technology, 16 Woomyeon-dong, Seocho-ku, Seoul 137-140, Korea

· 논 문 번 호 : 20001104-04S
· 수정완료일자 : 2000년 12월 20일

band. In this structure, the size and weight of the components are significantly reduced compared with those of the conventional resonators made by metallic cavities, while demonstrating an increased quality factor when compared with other planar resonators.

Ⅱ. THE PRINCIPLE OF MEMS CAVITY RESONATOR

2-1 Theoretical analysis

Fig. 1 shows the schematic of the two-port cavity resonator, which is one of the structures discussed in this paper. The rectangular cavities to be represent a significant section in many practical radio-frequency system. The important parameters in the rectangular cavity include field configurations that can be supported by such structures and their corresponding cut-off frequency, guided wavelengths, and quality factor Q, which is very attractive characteristics of the rectangular cavities. The rectangular waveguide cavity is formed by taking a section of a waveguide and enclosing its front and back faces with conducting plates, as shown in Fig. 2.

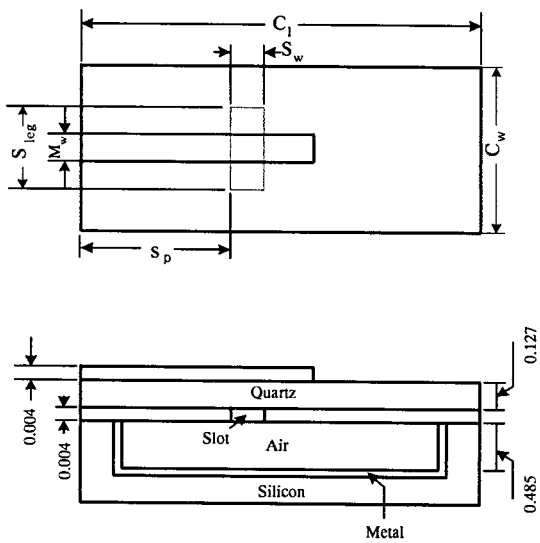

Fig. 1. The schematic of the two-port cavity resonator.

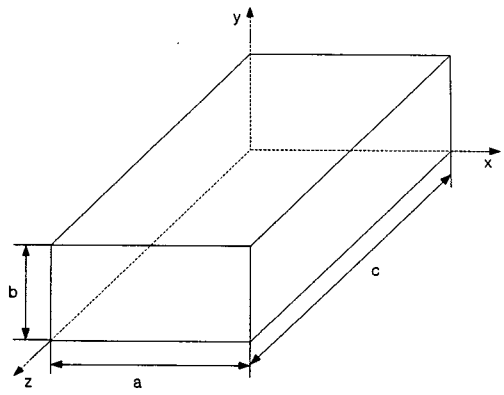

Fig. 2. Geometry for the rectangular cavity.

The field configuration inside a rectangular cavity may be either TE or TM mode. Since transverse electric (to z) modes for rectangular cavity must be derived in a manner similar to those of a rectangular waveguide, except those standing wave functions.

The resonant frequency for the TE^{z}_{mnp} mode is given by

$$(f_r)^{TE}_{mnp}=\frac{1}{2\pi\sqrt{\mu\varepsilon}}\sqrt{\left(\frac{m\pi}{a}\right)^2+\left(\frac{n\pi}{b}\right)^2+\left(\frac{p\pi}{c}\right)^2} \tag{1}$$

The transverse field components of the TE_{mn} mode can be represented in the below equation.

$$E_x=\frac{j\omega\mu n\pi}{k_c^2 b}A_{mn}\cos\frac{m\pi x}{a}\sin\frac{n\pi y}{b}e^{-j\beta z} \tag{2}$$

$$E_y=\frac{-j\omega\mu m\pi}{k_c^2 a}A_{mn}\sin\frac{m\pi x}{a}\cos\frac{n\pi y}{b}e^{-j\beta z} \tag{3}$$

$$H_x=\frac{j\beta m\pi}{k_c^2 a}A_{mn}\sin\frac{m\pi x}{a}\cos\frac{n\pi y}{b}e^{-j\beta z} \tag{4}$$

$$H_y=\frac{j\beta n\pi}{k_c^2 b}A_{mn}\cos\frac{m\pi x}{a}\sin\frac{n\pi y}{b}e^{-j\beta z} \tag{5}$$

where, the propagation constant is given by

$$\beta=\sqrt{k^2-k_c^2}=\sqrt{k^2-\left(\frac{m\pi}{a}\right)^2-\left(\frac{n\pi}{b}\right)^2} \tag{6}$$

Here $k_c^2=k^2-\beta^2$ is the cutoff wavenumber.

In addition to its resonant frequency, one of the most important parameters of a resonant cavity is its

quality factor Q.

$$Q = \omega \frac{W_t}{P_d} = \omega \frac{W_e + W_m}{P_d} \tag{7}$$

where, P_d represents the dissipated power, and W_e and W_m is the electric and magnetic stored energy.

The quality factor for TE_{101} mode rectangular cavity can be represented in a following equation.

$$(Q)_{101}^{TE} = \frac{\pi\eta}{2R_s}\left[\frac{b(a^2+c^2)^{2/3}}{ac(a^2+c^2)+2b(a^3+c^3)}\right] \tag{8}$$

where, R_s is the surface resistance.

Therefore, the quality factor of the only rectangular cavity presented in this paper can be found to be about 7800, which means the unloaded quality factor. To take into account the effects of input and output loading in the two-port micromachined cavity resonator, the quality factor of the structure can be broken down into different figures of merit, namely the loaded Q, the unloaded Q, and the external Q. The loaded Q is the measured quality factor taking into account the loading effects of the resonator itself and also the loading of the external circuit[4]. As a matter of fact, only loaded Q of a resonator can actually be measured. For a resonator in bandpass configuration with a resistive matched source and load impedance, the loaded quality factor can be obtained from measuring the 3 dB bandwidth of the S_{21} (S_{11}) as shown below equation.

$$Q_L = \frac{f_0}{\Delta f_{3dB}} \tag{9}$$

Here, f_0 is the resonant frequency and Δf_{3dB} is the 3 dB bandwidth of the S_{21} (S_{11}) response. The external Q can then be obtained from the loaded Q and the insertion loss of the resonator at the resonant frequency by solving as shown in the following equation.

$$Q_{ext} = \frac{Q_L}{S_{21}(f_0)} \tag{10}$$

where $S_{21}(f_0)$ is the transmission coefficient at resonance for the bandpass resonator and is measured in linear scale.

The three definitions for the quality factor for both the bandpass and the bandstop configurations are given by

$$\frac{1}{Q_U} = \frac{1}{Q_L} - \frac{1}{Q_{ext}} \tag{11}$$

2-2 The analysis of the cavity resonator's parameters

To solve the manufacturing tolerance problems, extensive analyses of the micromachined cavity resonator have been performed for the effects of variety of factors, such as the position of the slot, the width and length of the slot, cavity thickness, and the quartz thickness. The finite-element method (FEM) is used to study the effect of variety of factors presented in this paper. This technique mainly uses the method of moments to analyze the open part of the structure and to compute the field inside the cavity[5]. The cavity and the microstrip lines are separated by the ground plane of the microstrip lines. The field inside or outside the cavity can be represented as an integral of the unknown equivalent current source. By enforcing the continuity of tangential magnetic fields across the slots, the current distribution on the microstrip lines and field distribution on the slots are derived by the FEM method. A comprehensive review of these investigation is discussed in the below.

First, the position of the slot controls the amount of coupling between the air cavity and the microstrip line. This paper presents the variations of the resonance frequency and loaded quality factor due to the position of the slot for the case of one port cavity resonator as shown in Fig. 3. From the figures, the resonant frequency for the cavity resonator decreases with increasing the position of slot (S_p) relative to the input port. Also, the loaded

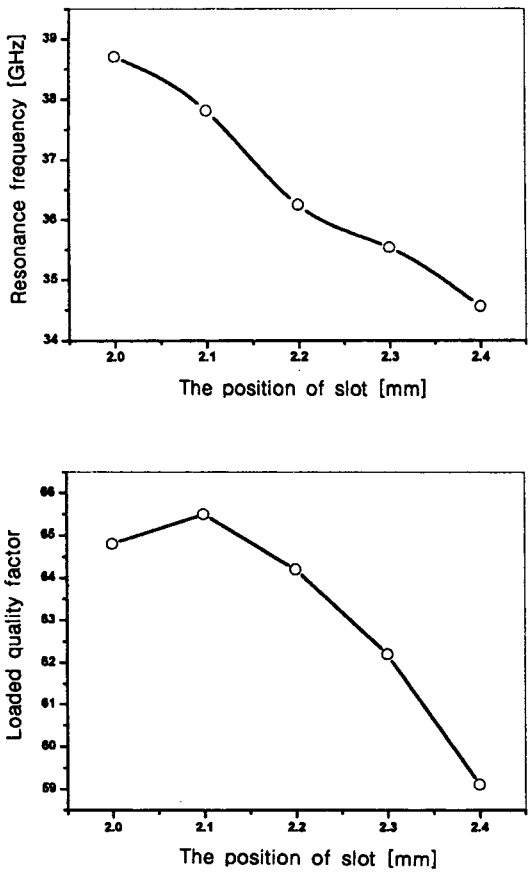

Fig. 3. Resonance frequency and Q versus the position of slot.

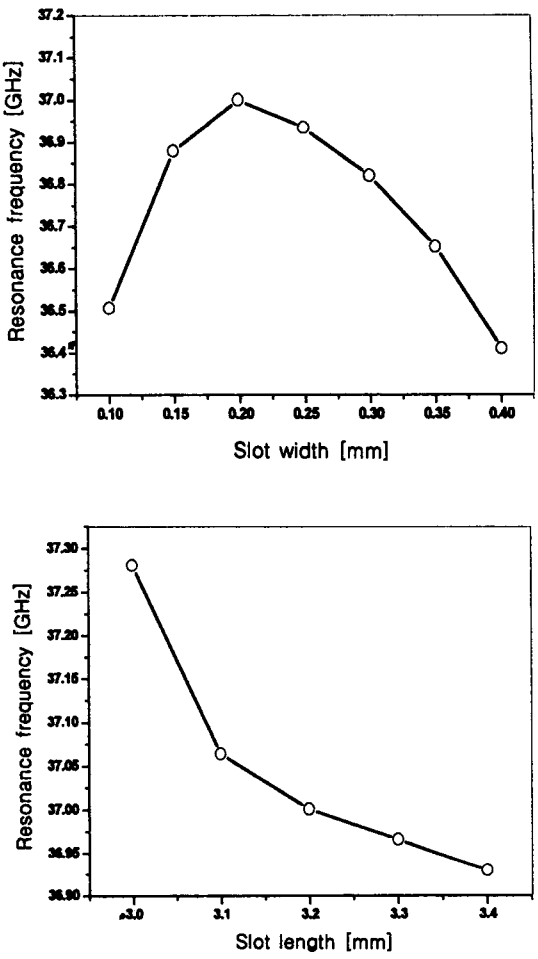

Fig. 4. Resonance frequency versus the slot width and length.

Q values increases a little, and then decreases with increasing the position of slot (S_p), because the magnitude of the magnetic field is decreased.

Second, the effect of slot length and width regarding to the resonant frequency of the cavity resonator is investigated and shown in Fig. 4. The resonant frequency of the cavity decreases with increasing slot length. As the slot length increases, even though there is high coupling between the microstrip line and the air cavity, it starts to support radiating mode in the slot. Therefore, the slot length has to be controlled without resonance caused by a slot mode. In the case of the 37 GHz two-port micromachined cavity resonator with the fixed slot length of 3400 μm, which is the optimum value in this case, the slot width has been varied from 100 μm to 400 μm. With this variation of slot width, the resonant frequency has the maximum value at the slot width of about 200 μm and decreases elsewhere.

Third, the size of the rectangular cavity is the parameter of deciding the resonant frequency, which is designated by a and c in Fig. 2. If the one port cavity resonator would be designed, the rectangular cavity is constructed as the TE_{101} mode, while it would be TE_{102} mode for the case of two-port resonator. Theoretically, the thickness of the rectangular cavity is represented as b in Fig. 2. The thickness should not affect the resonant frequency of the

dominant mode in the rectangular cavity. However, the simulation result using the FEM method has been turned out that the resonant frequency and the insertion loss characteristics depend on the cavity thickness, as shown in Fig. 5. In other words, as the cavity thickness is increased, the resonant frequency moves to the higher frequency region.

As the result of the FEM calculation about the insertion loss, the insertion loss is reduced, if the cavity thickness is increased. However, the limitation of the cavity thickness is made by the substrate thickness and the bulk etching capability. In this paper, the cavity is fabricated on a silicon wafer with the thickness of 640 μm by using wet etching until a depth of about 485 μm is achieved.

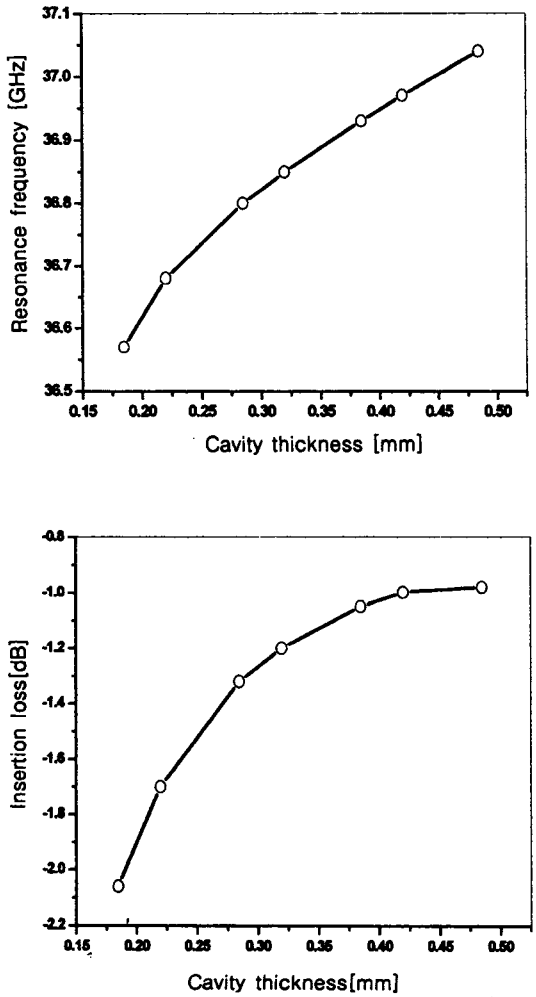

Fig. 5. Resonance frequency and insertion loss versus cavity thickness.

Fourth, the magnetic coupling between microstrip line and slot has been maximized by the dielectric constant of the substrate of the microstrip line. Theoretically, the coupling methods consist of the electric and magnetic coupling. The dielectric constant of the substrate is the main parameter to control the magnitude of magnetic coupling between the microstrip line and coupling slot. This paper represents the magnitude of the magnetic coupling as the electric charge Q_0, which consists of Q_{01} and Q_{02}. Q_{01} denotes the electric charge in the homogeneous dielectric medium (quartz in this paper) between the microstrip line and the metal ground, and relates to the magnetic coupling into the cavity. Q_{02} denotes the electric charge in the inhomogeneous dielectric medium, which means the surface charge between the quartz and air. The variation of the normalized electrical charge depending on the dielectric constant of the quartz substrate is shown in Fig. 6. From this figure, as the dielectric constant of the homogeneous medium is increased, the normalized electric charge (Q_{01}) is reduced, and thus the amount of magnetic coupling into the cavity is reduced.

Fifth, the thickness of the dielectric medium has

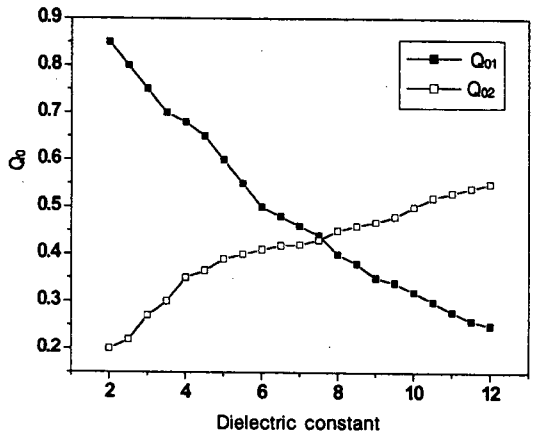

Fig. 6. The electric charge, Q vs. the dielectric constant.

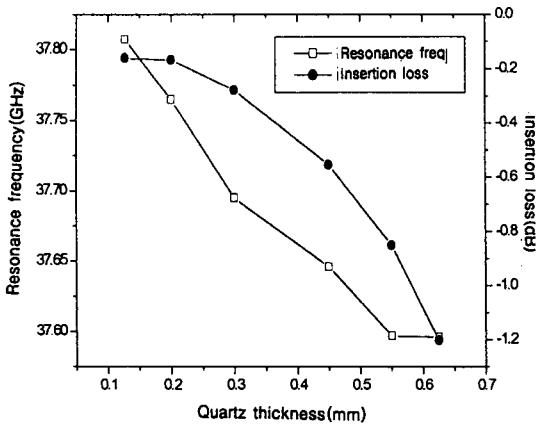

Fig. 7. The resonant frequency and insertion loss versus the quartz thickness.

been related with the insertion loss and the resonant frequency of the two-port resonator. The values of the insertion loss and resonant frequency due to the variation in dielectric thickness from 100 μm to 700 μm, are investigated as shown in Fig. 7. From the figure, when the quartz thickness is increased, the resonant frequency of the cavity moves toward a little higher frequency and the insertion loss is increased correspondingly.

Ⅲ. FABRICATION

3-1 The fabrication of the cavity resonator

The cavity resonator is fabricated using micro-machining techniques. In recent years, with an extensive development of the RF MEMS(Micro-Electro-Machnical System) design, some fabrication techniques such as the bulk and surface micro-machining techniques have been introduced. In this paper, the micromachined one- and two-port cavity resonators have been fabricated in silicon substrate with the thickness of 500 μm using micromachining etching techniques. This technique includes the cavity process by wet etching, and the slot and microstrip formations by the conventional photo-lithography.

First, SiNx with the thickness of 1800 Å has been deposited on the 640 μm thick silicon substrate using LPCVD (Low Pressure Chemical Vapor Deposition) (Fig. 8-a). After the wet etching mask patterning using IPC (Fig. 8-b), the silicon wafer has been etched until a depth of about 485 μm is achieved using KOH, which is the silicon etchant (Fig. 8-c). Once the wafer is etched, it is metallized with a total thickness of 2 μm. To plate the ground metal, Al with 300 Å thickness, Au, 700 Å thickness have been sticked on the silicon wafer, using the sputtering technique, and then gold electro-plated with a total thickness of 1.5 μm (Fig. 8-d).

Second, the fabrication of microstrip line and slot is achieved on the quartz substrate with 125 μm thickness. The two microstrip lines are gold electro-plated with a total thickness of 4 μm in order to minimize transmission line loss. One side of the Quartz substrate to make the microstrip line has been sticked with the sputter technique using Ti, with the thickness of 300 Å, and Au with the thickness of 700 Å, and then, gold plated with a total thickness of 4.0 μm (Fig. 9-a). The other side of the quartz substrate is plated with Al, 5000 Å thickness using the sputtering technique (Fig. 9-b). To pattern the slot, Al has been etched with AL-12 etchant (Fig 9-c).

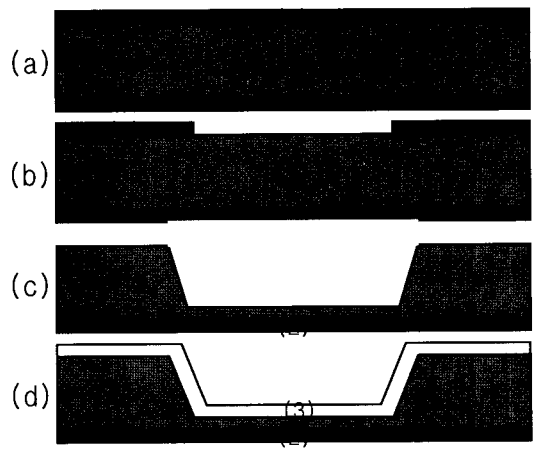

Fig. 8. Schematic for the cavity process on Si substrate.

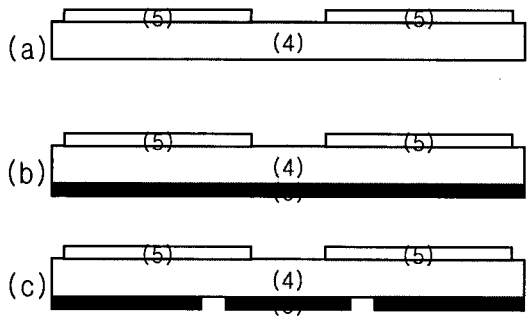

Fig. 9. Schematic for the formation of microstrip feeding lines and slot on quartz wafer.

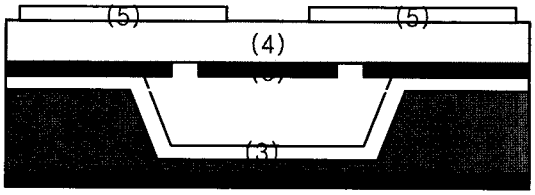

Fig. 10. Schematic for wafer bonding between Si and Quartz.

The last step is that two wafers of the silicon and quartz are then bonded together with silver epoxy as shown in Fig. 10.

3-2 SEM photographs

Fig. 11 (a) shows the SEM photograph of the interior of the silicon substrate. From the figure, the metallized cavity is observed to be steep and clear. Fig. 11 (b) shows the SEM photograph of the microstrip line on the quartz substrate which is bonded with Si substrate. The slot exists across the microstrip line on back side of the quartz (not shown in the picture). The CPW-to-Microstrip transition adaptor, Probepoint 0503^{TM} chip is connected with the microstrip by wedge bonding for the on-wafer characterization.

Ⅳ. CHARACTERIZATION

For the characterization of the micromachined

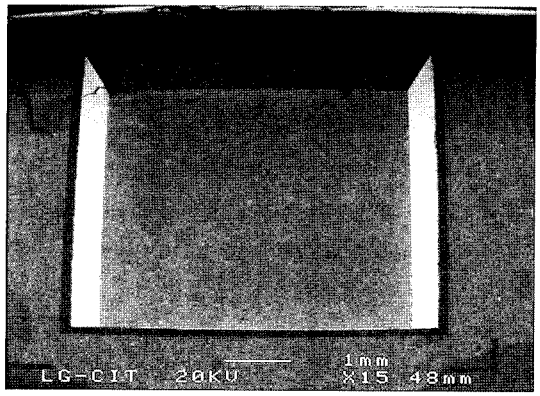

(a)

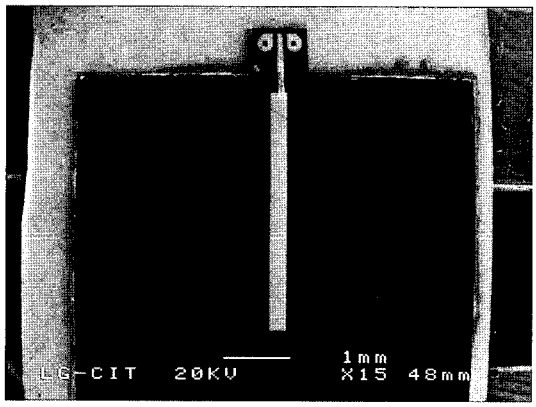

(b)

Fig. 11. SEM photographs for the micromachined cavity resonator.

cavity resonator with GSG probe, which is matched to the characteristic impedance of 50 Ω, the microstrip to CPW transhition is needed.

In this experiment, a CPW-to-microstrip transition adapter, Probepoint 0503^{TM} from Jmicro Technology is used to measure the S-parameters for the one- and two-port cavity resonator[6]. This ciruit works as a CPW-to-microstrip transition adaptor without loss up to 40 GHz. The connection between the adaptor and the micromachined cavity resonator has been done by gold wire bonding.

The micromachined cavity resonators have been characterized by an HP 8510C network analyzer.

4-1 One-port cavity resonator

The micromachined cavity resonator has been designed by HP HFSS^{TM} ver. 5.5, which is a 3-D microwave simulaion tool. Fig. 12 exhibits the simulation result for the resonant frequency of 37 GHz. With the expectation of frequency shift after fabrication, it is practically designed with the resonant frequency of 36.3 GHz, which is shifted toward lower band about 700 MHz. The return loss is about 32 dB.

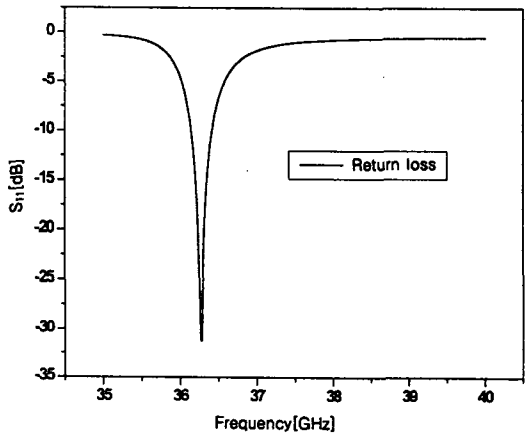

Fig. 12. The simulation result of the one-port cavity resonator.

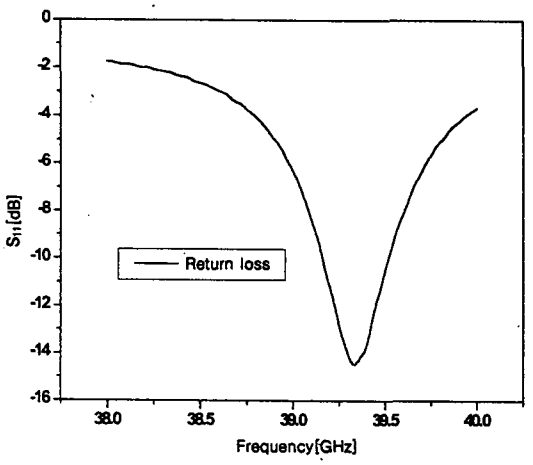

Fig. 13. The measurement result of the one-port cavity resonator.

Fig. 13 shows the measurement result of the micromachined one-port cavity resonator. This resonator has been measured by an HP 8510C Network Analyzer. The measured resonant frequeny is shown to be 39.34 GHz, which is shifted toward upper band about 3 GHz.

The difference between the simulation and measurement result is maybe due to the fabrication margin and wire bonding effects at the output port.

4-2 Two-port cavity resonator

Also, two-port cavity resonator is designed with the 3-D computed simulation, fabricated on Si and quartz wafer, and the S-parameters are measured through an HP 8510C network analyzer. The two slots to make the magnetic coupling are located at about 1/4 and 3/4 of the length of the cavity. Fig. 14 shows the simulation results for the resonator with the resonant frequency of 37.8 GHz with the expectation of fabrication margin.

The unloaded quality factor of a micromachined cavity resonator can be obtained from Eq. (12).

$$Q_U = \omega \frac{W_m + W_e}{P_l} \tag{12}$$

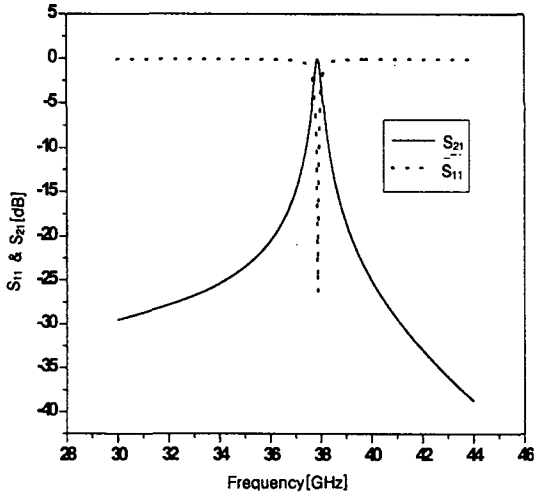

Fig. 14. The simulation result of two-port cavity resonator.

where W_m and W_e are the energies stored in the magnetic and electric fields respectively, and P_l is the net power dissipated. In the case of the air filled cavity, the net power dissipated is purely the ohmic loss from the currents on the sides of the resonator. By neglecting the effects of the non-vertical side-walls, which is caused from fabrication process, the imperfection in bonding wire, and the CPW-tomicro-strip transition, the quality factors for different resonators can be easily calculated using the FEM method for a given cavity. The unloaded quality factor for a 37.8 GHz two-port resonator is 2390 for the TE^{102} mode using the conductivity of gold as $3.9\times10^{7}\Omega^{-1}$ m^{-1}.

The measurement result for the two-port micro-machined cavity resonator is shown in Fig. 15. The resonant frequency is observed to be 39 GHz, which is shifted toward upper band about 1.2 GHz compared with the simulation result. The difference between the simmulation and measurement results is believed to be due to the fabrication margin of the slot position and the impedance mismatch at the output port. S_{11} and S_{21} at the resonance are found to be 19.8 dB and -4.6 dB, respectively. The insertion loss is much worse than that of simulation data (about 0.1 dB). This is mainly due to the process

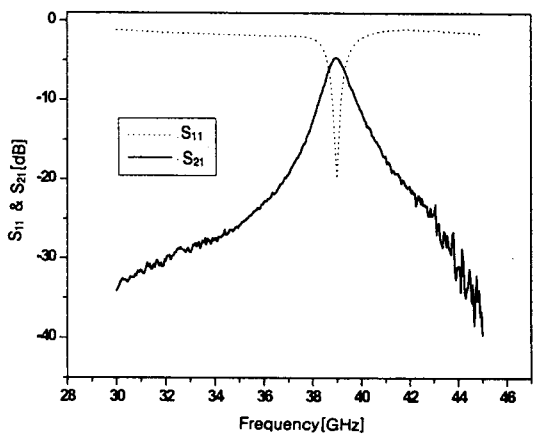

Fig. 15. The measurement result of two-port resonator.

error such as surface flatness, the position of the slot, and wafer bonding between the quartz and silicon by silver epoxy.

The loaded Q of 44.3 and then unloaded Q of 107 are calculated for the two-port cavity resonator. It is believed that the big difference in insertion loss between the measurement and simulation leads to the much smaller value of unloaded Q in measurement compared with that of simulation (2400).

V. CONCLUSION

In this paper, design parameters for the millimeter wave cavity resonators have been fully discussed. Also, one-port and two-port cavity resonator at mill-imeter wave range have been designed with the 3-D simulator and fabricated. The use of Si micro-machining technique enables integration of a cavity resonator with microstrip line without affecting the planar characteristic of the circuit. The size and weight of the micromachined cavity resonator are significantly reduced compared with the conventional resonators made by metallic cavity.

One-port resonator shows the resonant frequency of 39.34 GHz, the return loss of 14.5 dB, and the loaded Q (Q_L) of 150. Two-port cavity resonator shows the resonant frequency of 39 GHz, the insertion loss of 4.6 dB, the loaded Q (Q_L) and unloaded Q (Q_U) of 44.3 and 107, respectively.

These cavity resonators are expected to be used as frequency tuning elements for the development of a low phase-noise millimeter wave oscillator or VCO.

REFERENCES

[1] H. H. Meinel, "Communication application of millimeter wave. History, present status and future trends," *IEEE Trans. Microwave Theory Tech.*, vol. 43, pp. 1639-1653, July, 1995.

[2] J. Burns, "The application of millimeter wave technology for personal communication networ-

ks in the United Kingdom and Europe: A technical and regulatory overview," *IEEE MTT-S Symp. Dig.*, pp. 635-638, 1994.

[3] J. Papapolymerou, J.-C. Cheng, J. East, and L. P. B. Katehi, "A micromachined high-Q X-band resonator," *IEEE Microwave and Guided Wave Lett.*, vol. 7, pp. 168-170, 1997.

[4] J. M. Guan and C. C. Su, "Resonant frequencies and field distributions for the shielded uniaxially anisotropic dielectric resonator by the FD-SIC method," *IEEE Trans. Microwave Theory Tech.*, vol. 45, pp. 1767-1777, Oct. 1997.

[5] K. S. Yee and J. S. Chen, "Impedance boundary condition simulation in the FDTD/FVTD hybrid," *IEEE Trans. Antennas Prop.*, vol. 45, pp. 921-925, June, 1997.

[6] *J-micro Technology Product Information,* Portland, 1994.

[7] A. R. Brown and G. M. Rebeiz, "A k-band micromachined low-phase-noise oscillator," *IEEE Trans. Microwave Theory Tech.*, vol. 47, pp. 1504-1508, Aug., 1999.

[8] Y. Kwon, C. Cheon, N. Kim, C. Kim, I. Song, and C. Song, "A Ka-band MMIC oscillator stabilized with the micromachined cavity," *IEEE Microwave and Guided Wave Lett.*, vol. 9, No. 9, pp. 360-362, Sept., 1999.

Ki-Jae Song

Refer to the issue of vol. 11. no. 8

Bup-Sang Yoon

2000. 2.: Dept. of Radio Science & Eng., Kwangwoon Univ. (B. S.)

2000. 3.~Present : Dept. of Radio Science & Eng., Kwangwoon Univ., Master Student

Research Interests : Microwave/Millimeter-wave active and passive devices, RF MEMS

Jong-Chul Lee

Refer to the issue of vol. 11. no. 8

Byungje Lee

Refer to the issue of vol. 11. no. 8

Jong-Heon Kim

Refer to the issue of vol. 11. no. 8

Nam-Young Kim

Refer to the issue of vol. 11. no. 8

Jae Y. Park

Refer to the issue of vol. 11. no. 6

Geun-Ho Kim

Refer to the issue of vol. 11. no. 6

Jong-Uk Bu

Refer to the issue of vol. 11. no. 6

Ki-Woong Chung

Refer to the issue of vol. 11. no. 6